

Accepted Manuscript

Identification of novel microsomal prostaglandin E₂ synthase-1 (mPGES-1) lead inhibitors from fragment Virtual Screening

Gianluigi Lauro, Michele Manfra, Silvana Pedatella, Katrin Fischer, Vincenza Cantone, Stefania Terracciano, Alessia Bertamino, Carmine Ostacolo, Isabel Gomez-Monterrey, Mauro De Nisco, Raffaele Riccio, Ettore Novellino, Oliver Werz, Pietro Campiglia, Giuseppe Bifulco

PII: S0223-5234(16)30773-5

DOI: [10.1016/j.ejmech.2016.09.042](https://doi.org/10.1016/j.ejmech.2016.09.042)

Reference: EJMECH 8908

To appear in: *European Journal of Medicinal Chemistry*

Received Date: 28 April 2016

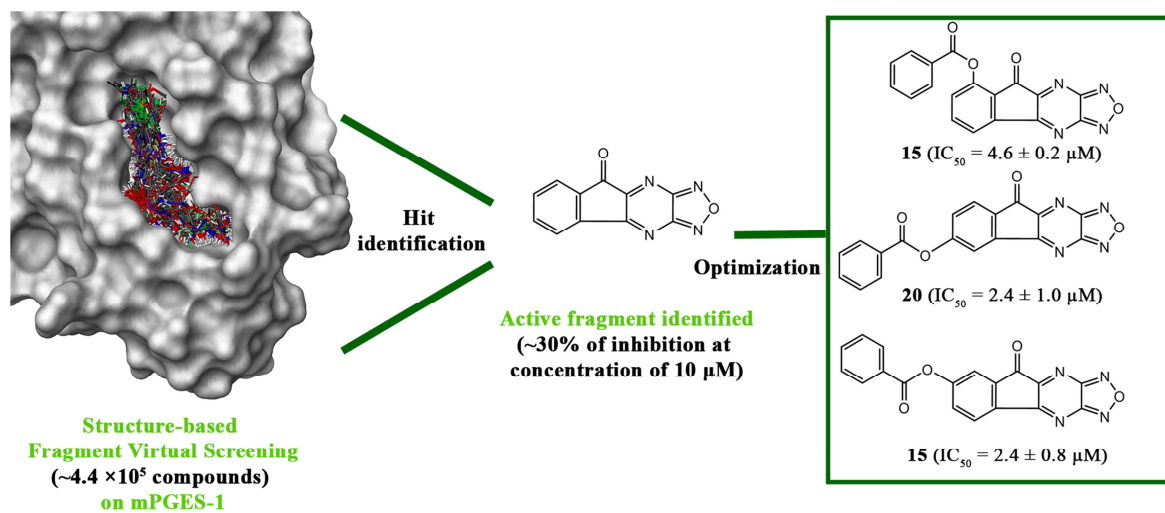
Revised Date: 1 July 2016

Accepted Date: 13 September 2016

Please cite this article as: G. Lauro, M. Manfra, S. Pedatella, K. Fischer, V. Cantone, S. Terracciano, A. Bertamino, C. Ostacolo, I. Gomez-Monterrey, M. De Nisco, R. Riccio, E. Novellino, O. Werz, P. Campiglia, G. Bifulco, Identification of novel microsomal prostaglandin E₂ synthase-1 (mPGES-1) lead inhibitors from fragment Virtual Screening, *European Journal of Medicinal Chemistry* (2016), doi: 10.1016/j.ejmech.2016.09.042.

This is a PDF file of an unedited manuscript that has been accepted for publication. As a service to our customers we are providing this early version of the manuscript. The manuscript will undergo copyediting, typesetting, and review of the resulting proof before it is published in its final form. Please note that during the production process errors may be discovered which could affect the content, and all legal disclaimers that apply to the journal pertain.





ACCEPTED MANUSCRIPT

Identification of novel microsomal prostaglandin E₂ synthase-1 (mPGES-1) lead inhibitors from Fragment Virtual Screening

Gianluigi Lauro,^a Michele Manfra,^b Silvana Pedatella,^c Katrin Fischer,^d Vincenza Cantone,^{a,d}
Stefania Terracciano,^a Alessia Bertamino,^a Carmine Ostacolo,^c Isabel Gomez-Monterrey,^c Mauro
De Nisco,^b Raffaele Riccio,^a Ettore Novellino,^c Oliver Werz,^d Pietro Campiglia,^{a,*} and Giuseppe
Bifulco^{a,*}

^aDepartment of Pharmacy, University of Salerno, via Giovanni Paolo II 132, 84084 Fisciano,
Italy

^bDepartment of Science, University of Basilicata, Viale dell'Ateneo Lucano 10, 85100 Potenza,
Italy

^cDepartment of Pharmacy, Università degli Studi di Napoli "Federico II", Via Montesano 49,
80131 Napoli, Italy

^dDepartment of Pharmaceutical/Medicinal Chemistry, Institute of Pharmacy, University of Jena,
Philosophenweg 14, D-07743 Jena, Germany

^eDepartment of Chemical Sciences, University of Napoli Federico II, Via Cintia 4, I-80126
Napoli, Italy

*To whom correspondence should be addressed: bifulco@unisa.it, Telephone: +39 (0)89 969741, Fax: +39 (0)89 969602, pcampiglia@unisa.it, Telephone: +39 (0)89 969242, Fax: +39 (0)89 969602

ACCEPTED MANUSCRIPT

ABSTRACT

Identification of new microsomal prostaglandin E₂ synthase-1 (mPGES-1) inhibitors is currently sought for the treatment of cancer and inflammation. Here we show the results of a Fragment Virtual Screening campaign using the X-ray crystal structure of human mPGES-1 (PDB code: 4AL0). Among the fragments selected and biologically tested, **6** (9H-indeno[1,2-b][1,2,5]oxadiazolo[3,4-e]pyrazin-9-one) showed the most promising mPGES-1 inhibitory activity (~30% inhibition at 10 μ M). A minimal structure-based optimization of **6** led to compounds **15**, **20** and **21**, with a promising enhancement of the inhibitory activity ($IC_{50} = 4.6 \pm 0.2 \mu$ M for **15**; $2.4 \pm 1.0 \mu$ M for **20**; $IC_{50} = 2.4 \pm 0.8 \mu$ M for **21**). The unprecedented chemical core and the possibility of synthesizing novel derivatives reveal a new and attractive field of action for the development of mPGES-1 inhibitors with potential anti-inflammatory and anticancer properties.

KEYWORDS: Molecular docking, cancer, inflammation, mPGES-1 inhibitors, Virtual Screening

Introduction

Nonsteroidal anti-inflammatory drugs (NSAIDs) nowadays represent the most important agents for the inflammation therapy. They act suppressing the biosynthesis of prostaglandins (PGs), bioactive mediators involved in key physiological functions but also in several other pathologic conditions, such as tumorigenesis[1]. The relationship between inflammation and tumor progression is noteworthy[2-4], and the correlation between inflammatory events and the development of pre-cancerous lesions at various anatomic sites has been established[5-7]. Proliferation, invasion and migration processes are promoted by inflammatory events and, indeed, the identification of new anti-inflammatory drugs could be synergic in the context of anti-cancer pharmacological strategies[8]. Nevertheless, NSAIDs cause several side effects due to their action on cyclooxygenase (COX) targets, such as cardiovascular, gastrointestinal and renal side[9], and then the development of safer alternatives especially for long-term therapies is even more required[10, 11].

In this scenario, prostaglandin E₂ synthases (PGES, namely mPGES-1, mPGES-2 and cPGES) represent valuable targets for the development of new anti-inflammatory/anticancer agents with reduced side effects. Specifically, PGES are terminal enzymes involved in the biosynthesis of the inflammatory lipid mediator PGE₂[12, 13]. In particular, while mPGES-2 and cPGES represent the constitutive form, the inducible membrane-bound isoform mPGES-1 has become as a key drug target in PGE₂-related acute and chronic disorders[14], such as pain[15], fever[16], rheumatoid arthritis[17], arthritis[18], inflammation[19], and cancer[20, 21]. Then, mPGES-1 inhibitors recently emerged as new valuable and safer drugs, avoiding the chemical conversion of PGH₂, enzymatically produced by the COXs, to PGE₂[22]. Up to now, a number of mPGES-1 inhibitors featuring different chemical platforms have been developed[23]. The structure-based

design of new inhibitors was supported in 2013 by the first X-ray crystal structure of the protein with the identification of the active site[24], and subsequently by other crystal structures with several known mPGES-1 inhibitors acting both as substrate (available crystal structures with PDB codes: 4BPM, 4WAB, 4YK5, 4YL0, 4YL1, 4YL3)[25-27] and substrate/cofactor competitors (PDB code: 4AL1)[24]. Also, new high-resolution X-ray structures of human mPGES-1 in complex with new and potent inhibitors have been presented (PDB code: 5BQG, 5BQH, and 5BQI)[28]. This new information is crucial in a medicinal chemistry approach for the structure-based design of novel inhibitors, and it could also serve to retrospectively analyze the binding modes of known binders[22].

In the last few years, our research group has been involved in the computer-aided design, chemical synthesis and biological evaluation of novel mPGES-1 inhibitors featuring different chemical scaffolds[29-39]. With the aim of identifying novel mPGES-1 featuring unprecedented molecular scaffolds, a Virtual Screening computational approach was undertaken using the recent crystal structure of mPGES-1 (PDB code: 4AL0). Specifically, we here focused on the fragment-based drug discovery (FBDD) approach[40], since it has recently emerged as a significant tool in the field of medicinal chemistry for discovery of new hit compounds. In fact, the identification of low-molecular-weight compounds (<300 Da) could allow the design of high affinity ligands following a “linking” or “growing” approach[37, 41]. Starting from these considerations, we report a Fragment Virtual Screening workflow leading to the identification of new valuable chemical scaffolds, whose biological activities were detected by *in vitro* experiments. Moreover, simple modifications on the most promising fragment prompted to the chemical synthesis of a small set of derivatives, whose remarkable inhibitory activities pave the way for the development of novel potent mPGES-1 inhibitors.

Materials and Methods

Input files preparation for molecular docking. The chemical structures of the investigated compounds were retrieved from the ZINC database [42, 43]. Specifically, we used the “Fragment-Like – In Stock” subset, then accounting the commercially available compounds for an immediate delivery. When the library was downloaded (2013), it was composed by $\sim 4.4 \times 10^5$ compounds. For the subsequent docking calculations, all the structures were converted in the .pdbqt format using OpenBabel software (version 2.3.2)[44], adding Gasteiger charges.

Protein 3D models were prepared using the Schrödinger Protein Preparation Wizard[45], starting from the mPGES-1 X-ray structure in the active form (PDB code: 4AL0)[24]. A first set of docking calculations was performed on the protein structure in absence of the cofactor GSH (named *mpges_1_no_gsh* branch), while it was preserved for a second set of experiments (*mpges_1_with_gsh* branch). Crystallized water molecules were removed, all hydrogens were added, and bond orders were assigned. Protein .pdb files obtained were then converted in .pdbqt format.

Molecular Docking. Docking calculations were performed using Autodock-Vina software[46]. In the configuration files linked to 3D structures of the proteins, we specified coordinates and dimensions along x,y,z axes of the grids related to the sites of presumable pharmacological interest. In particular, we chose the binding site between A and B chains for both the forms of the protein, and a grid box size of 24×20×18 and centered at 10.304 (x), -11.033 (y), and -8.384 (z), with spacing of 1.0 Å between the grid points, setting the exhaustiveness value to 8. For all the

investigated compounds, all open-chain bonds were treated as active torsional bonds. Docking results were analyzed with Autodock Tools 1.5.7 and Maestro (version 10.2)[45]. Illustrations of the 3D models were generated using VMD software[47] and Maestro (version 10.2)[45].

General Synthetic Information.

Materials. Inorganics, organic reagents, and solvents were commercial pure compounds and used without further purification. TLC analyses were performed using silica gel plates (silica gel 60 F-254) visualized by UV light, fluorescent light, and iodine. Column chromatography was carried out on silica gel (70-230 mesh). ^1H and ^{13}C NMR spectra were recorded on Varian Inova 500 MHz, BrukerAvance 400 MHz, and BrukerDrx 400 MHz spectrometers: chemical shifts in ppm (δ) and J coupling constants in Hz. The following abbreviations are used to indicate the multiplicity: s, singlet; d, doublet; m, multiplet; b, broad signal. Abbreviations, NBS: *N*-bromosuccinimide; DMSO: dimethylsulfoxide.

Synthesis of Compound 18. Substituted phenol **17** (296 mg, 2 mmol) was dissolved in 3 ml of 10% aqueous sodium hydroxide solution in a 25 mL flask. Solutions of tetra-*n*-butylammonium chloride (56 mg, 0.2 mmol) in 0.7 mL of dichloromethane and acyl chloride (232 μL , 2 mmol) in 2 mL of dichloromethane were prepared. After cooling all solutions at 0 °C, they were mixed at once. The reaction mixture was kept under vigorous magnetic stirring at 0 °C for 15 min and then poured over 50 mL of icy water. The organic layer was separated and the aqueous layer was extracted twice with 40 mL of diethyl ether. The combined organic extracts were washed with saturated NaCl solution. After drying on Na_2SO_4 , the solvent was evaporated, and the residue was purified by silica gel chromatography (CH_2Cl_2) to give the compound **18**. (456 mg; 1.8 mmol; 90%). ^1H NMR (400 MHz, CDCl_3): δ 7.83 (d, $J = 8.3$ Hz, 1H), 7.49-7.40 (m, 3H), 7.35-

7.26 (m, 4H), 3.19 (t, $J = 5.5$ Hz, 2H), 2.75 (t, $J = 5.5$ Hz, 2H). ^{13}C NMR (125 MHz, CDCl_3): δ 206.5, 164.6, 156.8, 156.0, 134.7, 133.9, 130.1, 128.8, 128.6, 125.0, 121.4, 119.7, 36.3, 25.6. Calculated for $\text{C}_{16}\text{H}_{12}\text{O}_3$: C, 76.18%; H, 4.79%; O, 19.03%; Found: C, 76.08%; H, 4.60%; N, 19.13%.

Synthesis of Compounds 13, 19. In a typical procedure, *N*-bromosuccinimide (671 mg, 3.6 mmol) was added to protected phenol (**12**, **18**) (456 mg, 1.8 mmol) in 9 mL of dimethylsulfoxide. The reaction mixture was stirred at 60 °C for 3 hours and then at 80 °C for 4 hours. The reaction mixture was cooled to room temperature and then poured into 200 mL of water. The product was extracted with three portions of 100 mL of dichloromethane, and then the combined organic extracts were dried (sodium sulfate), filtered and evaporated. The residue was purified by silica gel chromatography (Etp:AcOEt 7:3) to yield compounds **13** and **19**.

Compound 13: 328 mg (1.1mmol; 60%). ^1H NMR (500 MHz, DMSO-d_6): δ 8.22-8.13 (m, 3H), 8.02-7.99 (m, 2H), 7.80 (t, $J = 7.7$ Hz, 1H), 7.68-7.65 (m, 2H), 7.59 (s, 2H, OH); ^{13}C NMR (125 MHz, DMSO-d_6): δ 198.7, 198.6, 164.0, 152.7, 145.5, 141.3, 136.5, 132.2, 129.6, 127.6, 125.9, 125.3, 123.0, 88.9. Anal. Calcd. for $\text{C}_{16}\text{H}_{10}\text{O}_6$: C, 64.43; H, 3.38. Found: C, 64.11; H, 3.57. *Compound 19:* 349 mg (1.2 mmol; 65%). ^1H NMR (400 MHz, DMSO-d_6): δ 8.19-8.09 (m, 3H), 8.02-7.95 (m, 2H, OH), 7.72 (t, $J = 6.4$ Hz, 1H), 7.66-7.56 (m, 4H). ^{13}C NMR (100 MHz, DMSO-d_6): δ 196.9, 196.3, 164.4, 157.6, 140.7, 136.6, 134.9, 131.8, 130.9, 128.8, 126.4, 117.6, 88.4. Anal. Calcd. for $\text{C}_{16}\text{H}_{10}\text{O}_6$: C, 64.43; H, 3.38. Found: C, 64.11; H, 3.57.

Synthesis of Compounds 15, 20, 21. In a typical procedure, a mixture of gem-diol (**13**, **19**) (149 mg, 0.5 mmol) and furazan-3,4-diamine (**14**) (50 mg, 0.5 mmol) in 1.5 mL of ethanol and 1.5 mL of glacial acetic acid was stirred at room temperature for 18 hours and then heated at reflux for 6 hours. The precipitated solid was filtered and washed with water to yield the compounds **15**, **20**

and **21**. *Compound 15*: 76 mg (0.22 mmol; 45%), ^1H NMR (400 MHz, DMSO- d_6): δ 8.31-8.21 (m, 3H), 8.11-8.01 (m, 1H), 7.91 (d, $J = 8.1$ Hz, 1H), 7.83 (dd, $J = 10.7, 4.2$ Hz, 1H), 7.74-7.66 (m, 2H). ^{13}C NMR (100 MHz, DMSO- d_6): δ 186.1, 165.8, 165.5, 164.3, 151.6, 150.0, 149.7, 139.1, 136.4, 134.0, 131.7, 131.6, 131.5, 130.5, 124.0, 117.5. Anal. Calcd. for $\text{C}_{18}\text{H}_8\text{N}_4\text{O}_4$: C, 62.80; H, 2.34; N, 16.27. Found: C, 62.72; H, 2.10; N, 16.08. *Compounds 20 and 21*: A mixture of compounds **20** and **21** in ratio 1:0.88 respectively (0.25 mmol; 50%) was purified by silica gel chromatography (Etp:AcOEt 7:3). *Compound 20*: ^1H NMR (500 MHz, DMSO- d_6): δ 8.45 (d, $J = 8.3$ Hz, 1H), 8.25-8.19 (m, 3H), 8.03 (dd, $J = 8.3, 1.9$ Hz, 1H), 7.85-7.78 (m, 1H), 7.71-7.64 (m, 2H). ^{13}C NMR (125 MHz, DMSO- d_6): δ 185.1, 164.7, 163.3, 161.7, 158.2, 153.6, 142.1, 138.3, 137.4, 135.1, 132.2, 130.6, 129.6, 128.8, 127.2, 118.9. Anal. Calcd. for $\text{C}_{18}\text{H}_8\text{N}_4\text{O}_4$: C, 62.80; H, 2.34; N, 16.27. Found: C, 62.63; H, 2.10; N, 16.10. *Compound 21*: ^1H NMR (500 MHz, DMSO- d_6): δ 8.35 (d, $J = 1.8$ Hz, 1H), 8.26-8.20 (m, 3H), 7.94 (dd, $J = 8.3, 1.8$ Hz, 1H), 7.84-7.78 (m, 1H), 7.70-7.63 (m, 2H). ^{13}C NMR (100 MHz, DMSO- d_6): δ 184.7, 165.6, 163.9, 162.2, 157.3, 155.7, 142.3, 138.3, 137.9, 135.9, 130.9, 130.5, 130.1, 129.7, 127.8, 118.4. Anal. Calcd. for $\text{C}_{18}\text{H}_8\text{N}_4\text{O}_4$: C, 62.80; H, 2.34; N, 16.27. Found: C, 62.59; H, 2.19; N, 16.09.

Synthesis of Compounds 16, 22, 23. In a typical procedure, protected compounds (**15**, **20**, **21**) (177 mg, 0.51 mmol) were dissolved in MeOH/THF (1:1) and stirred with sodium thiophenolate (101 mg, 0.77 mmol). The reaction was heated to reflux for 2.5 h and precipitated solid was filtered and purified by silica gel chromatography (CH_2Cl_2) to yield compounds **16**, **22**, and **23**. *Compound 16*: 115 mg (0.48 mmol; 95%). ^1H NMR (500 MHz, DMSO- d_6): δ 7.85-7.72 (m, 1H), 7.63-7.54 (m, 1H), 7.26-7.18 (m, 1H). ^{13}C NMR (100 MHz, DMSO- d_6): δ 184.1, 165.5, 152.3, 149.3, 148.2, 141.1, 138.2, 136.1, 128.0, 124.5, 117.6. Anal. Calcd. for $\text{C}_{11}\text{H}_4\text{N}_4\text{O}_3$: C, 55.01; H, 1.68; N, 23.33. Found: C, 55.12; H, 1.88; N, 23.03. *Compound 22*: 115 mg (0.48 mmol; 95%).

^1H NMR (500 MHz, DMSO- d_6): δ 8.31 (s, 1H), 7.94 (d, $J = 8.5$ Hz, 1H), 7.20 (d, $J = 7.8$ Hz, 1H). ^{13}C NMR (100 MHz, DMSO- d_6): δ 183.0, 167.9, 163.6, 162.5, 153.7, 142.8, 133.2, 128.1, 124.5, 115.8. Anal. Calcd. for $\text{C}_{11}\text{H}_4\text{N}_4\text{O}_3$: C, 55.01; H, 1.68; N, 23.33. Found: C, 55.19; H, 1.89; N, 23.01. **Compound 23**: 115 mg (0.48 mmol; 95%). ^1H NMR (400 MHz, DMSO- d_6): δ 8.59 (bs, 1H, OH), 8.15 (d, $J = 6.2$ Hz, 1H), 7.37 (d, $J = 6.2$ Hz, 1H), 7.26 (bs, 1H). ^{13}C NMR (125 MHz, DMSO- d_6): δ 187.4, 167.5, 165.1, 164.3, 156.0, 155.9, 145.4, 135.9, 128.7, 128.4, 112.5. Anal. Calcd. for $\text{C}_{11}\text{H}_4\text{N}_4\text{O}_3$: C, 55.01; H, 1.68; N, 23.33. Found: C, 55.08; H, 1.97; N, 23.05.

Bioactivity assays

Cell-free mPGES-1 activity assay

Microsomes of IL-1 β -stimulated A549 cells were used as a source for mPGES-1. Expression of mPGES-1, preparation of microsomes and determination of mPGES-1 activity was performed as described previously[48]. In brief, A549 cells were treated with IL-1 β (1 ng/ml) for 48 h, cells were harvested, sonicated and the homogenate was subjected to differential centrifugation at a) 10,000 \times g for 10 min and b) 174,000 \times g for 1 h at 4 $^\circ\text{C}$. The microsomal fraction (pellet) was resuspended in 1 ml homogenization buffer (0.1 M potassium phosphate buffer, pH 7.4, 1 mM phenylmethanesulfonyl fluoride, 60 $\mu\text{g}/\text{mL}$ soybean trypsin inhibitor, 1 $\mu\text{g}/\text{mL}$ leupeptin, 2.5 mM glutathione, and 250 mM sucrose), the total protein concentration was determined, and microsomes were diluted in potassium phosphate buffer (0.1 M, pH 7.4) containing 2.5 mM glutathione. Test compounds (or DMSO as vehicle) were added, and after 15 min at 4 $^\circ\text{C}$ reaction (100 μl total volume) was initiated by addition of 20 μM PGH $_2$. After 1 min at 4 $^\circ\text{C}$, 100 μl of stop solution (40 mM FeCl $_2$, 80 mM citric acid, and 10 μM 11 β -PGE $_2$) were added. PGE $_2$ was separated by solid-phase extraction and analyzed by RP-HPLC as described previously[48].

Results and Discussion

Structural information. mPGES-1 is a glutathione-dependent membrane protein located on the endoplasmic reticulum and structurally organized as homotrimer, with three equivalent active site cavities within the membrane-spanning region at each monomer interface[24]. Each asymmetric monomer is characterized by a four-helix bundle motif, while each active site is toward the cytoplasmic part of the protein, between the N-terminal parts of helix II and IV of one monomer and the C-terminal part of helix I and the cytoplasmic domain of the adjacent monomer (Figure 1).

The analysis of the mPGES-1 crystal structure (PDB code: 4AL0)[24] disclosed several regions in the binding site that could be conveniently targeted by a functionalized ligand (Figure 1). Firstly, a binding groove is between the GSH binding site and a molecular surface nearby the cytoplasmic part of the protein, mainly composed by aromatic (B:Phe44, B:His53) and polar (B:Arg52) residues (colored in cyan, Figure 1).

A potential binder could establish π - π contacts with these aromatic groups, as occurred for the co-crystallized LVJ[25], 4DV, 4DZ, 4U8, 4U9[26], and as we proposed for dihydropyrimidin-2(1*H*)-one based mPGES-1 inhibitors[36].

The cofactor (GSH) is in a profound cavity mainly characterized by polar residues, and it adopts a U-shape due to the strong interactions between its two terminal carboxylic functions and the positively charged residues in the deeper part of the binding site (B:Arg38, A:Arg73) (colored in yellow, Figure 1). Importantly, the phenol group in the side chain of A:Tyr130 is involved in a π -stacking with the gamma peptide linkage between the cysteine and the glutamate

of GSH. This key residue could be targeted by a binder through a π - π interaction and/or polar/H-bond interactions with the phenol hydroxyl moiety in the side chain.

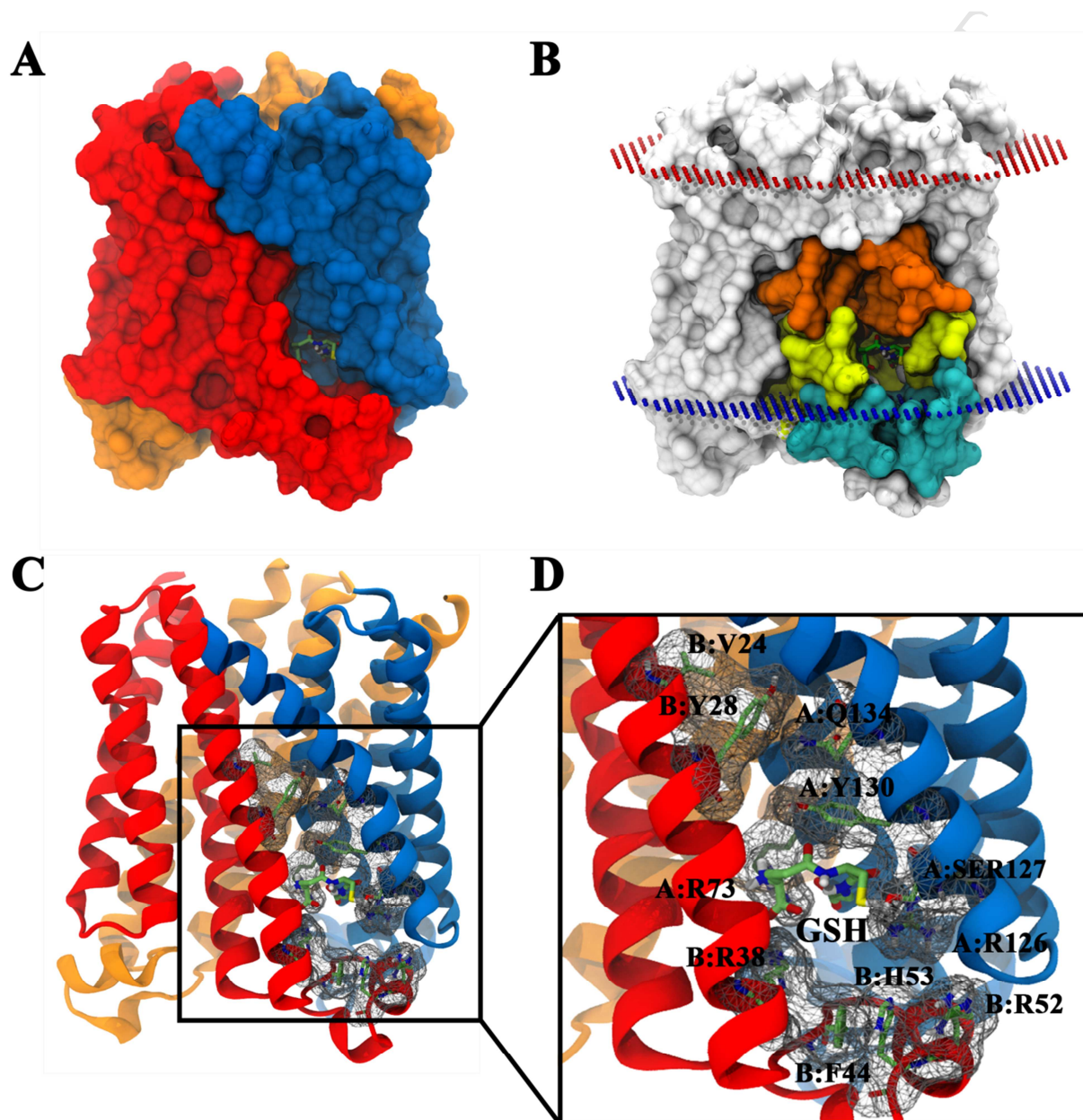


Figure 1. mPGES-1 structure: a) molecular surface representation of the mPGES-1 trimer (chain A blue, chain B red, chain C orange); b) molecular surface focused on the mPGES-1 binding site colored in orange, yellow, and cyan (see text for details), dummy atoms define the external part of endoplasmic reticulum membrane (above red atoms) and cytoplasmic (below blue atoms) sides; c,d) secondary structure focused to the mPGES-1 binding site (chain A

blue, chain B red, chain C orange); glutathione (GSH) cofactor and key-residues in the mPGES-1 binding site are represented in sticks (C: green, O red, N, blue, H light gray). (2-column fitting image)

Moreover, Ser127 on chain A represents another fundamental residue, since it was supposed to be involved in the catalytic process behind the isomerization of PGH₂ to PGE₂[24]. Finally, moving from the external part of endoplasmic reticulum membrane to the cytoplasmic part of the protein, a binding groove is identifiable at the intersection between helix 1 of chain B and helix 4 of chain A, with polar (A:Gln134), aliphatic (B:Val24) and aromatic (B:Tyr28) residues, and could be bound by long molecular functions (colored in orange, Figure 1).

Fragment Virtual Screening and biological evaluation. The identification of novel mPGES-1 inhibitors was conducted following a multi-step structure-based Fragment Virtual Screening approach, using the information arising from the analysis of the protein crystal structure crystallized by Sjögren et al. (PDB code: 4AL0)[24]. In a previous study, we have compared different mPGES-1 protein crystal structures highlighting the limited induced fit of the protein after ligand binding, and the applicability of semi-flexible molecular docking experiments (namely ligands considered as flexible, while protein as rigid)[37]. The workflow is represented in Figure 2.

The fragment library was docked onto the mPGES-1 protein structure after removal of the cofactor (glutathione, GSH; this branch was named *mpges_1_no_gsh*). After several selection steps (Steps 2-4, Figure 2), the most promising compounds were also docked on the protein in the presence of the cofactor (*mpges_1_with_gsh* branch) (Step 5, Figure 2).

Previous studies[49] highlighted that mPGES-1 inhibitors could bind the protein either occupying only the substrate binding site (prostaglandin H₂, PGH₂) or partially displacing GSH, then filling part of the cofactor binding site as far as extending to the substrate active site. These

two different binding modes seem to dramatically affect the potency, and in particular the accommodation in both the sites (substrate and cofactor sites) could lead to high affinity inhibitors[49]. Even if it is unlikely that a low affinity compound (such as a fragment) could interfere with the binding of the cofactor, we considered this possibility *in silico* in view of the subsequent optimization steps aimed to the generation of small molecules starting from fragments.

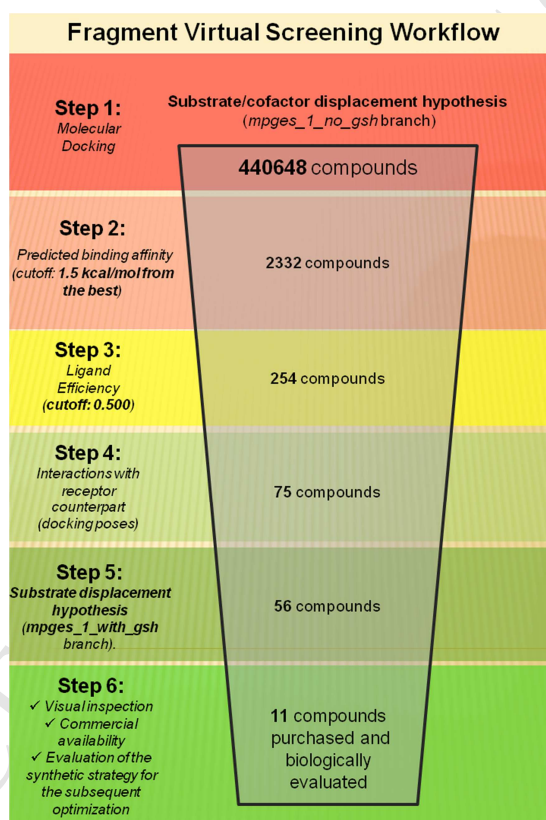


Figure 2. Fragment Virtual Screening workflow for the identification of novel mPGES-1 inhibitors (**1-column fitting image**)

The identification of the most promising binding poses represented the starting point for the design of optimized compounds, able to bind this protein form with high affinity respecting the

original fragment positions and filling the unoccupied regions thanks to the additional chemical groups. On the other hand, in order to facilitate the identification of active fragments prone to the optimization, we also evaluated the binding mode of the identified hits in the presence of GSH (*mpges1_with_gsh* branch), then finally selecting the compounds able to advantageously bind the protein in both the forms.

In details, the Virtual Screening workflow started with the molecular docking of the starting fragment library ($\sim 4.4 \times 10^5$ compounds) on the mPGES-1 protein structure built removing the cofactor (*mpges_1_no_gsh*). The first selection filter concerned the most energetically favored compounds, saving all the fragments whose predicted binding energies were comprised in a range of 1.5 kcal/mol from the best identified value (Step 2, Figure 2). For the selected fragments (2332 compounds), the related Ligand Efficiency[50] values were computed. This parameter links the estimated binding energy with the molecular size and could advantageously guide the optimization process of small chemical probes, leading to potent small molecules respecting the Lipinsky rules[51]. Compounds with Ligand Efficiency values better than -0.500 kcal/mol passed this filter, then restricting the number to 254 promising molecules (Step 3, Figure 2). In view of the subsequent step of fragment-to-lead optimization, we carefully analyzed the binding modes of the identified fragment docking poses, with the aim of selecting only those respecting the key interactions with the receptor counterpart. The selected fragments were supposed to advantageously interact in the cofactor (GSH) binding site, respecting part of the contacts detected for the cofactor in the protein structure. In particular, different set of ligand-receptor contacts were considered (Step 4, Figure 2):

- π - π interaction with A:Tyr130;
- polar contacts with A:Arg126 and/or B:Arg38 and/or A:Arg73.

Depending on the starting positions in the cofactor binding site, the fragments could be optimized using a “growing” approach on the cytoplasmic part (e.g. C-domain) or toward the external binding groove (A:Gln134, B:Val24, B:Tyr28) belonging to the mPGES-1 binding site. After that, the identified fragments (75 compounds) were then submitted to another docking round, considering the protein form in the presence of the cofactor (*mpges_1_with_gsh* branch) and evaluating their binding mode (Step 5, Figure 2). In this case, the following groups of interactions were set for the selection:

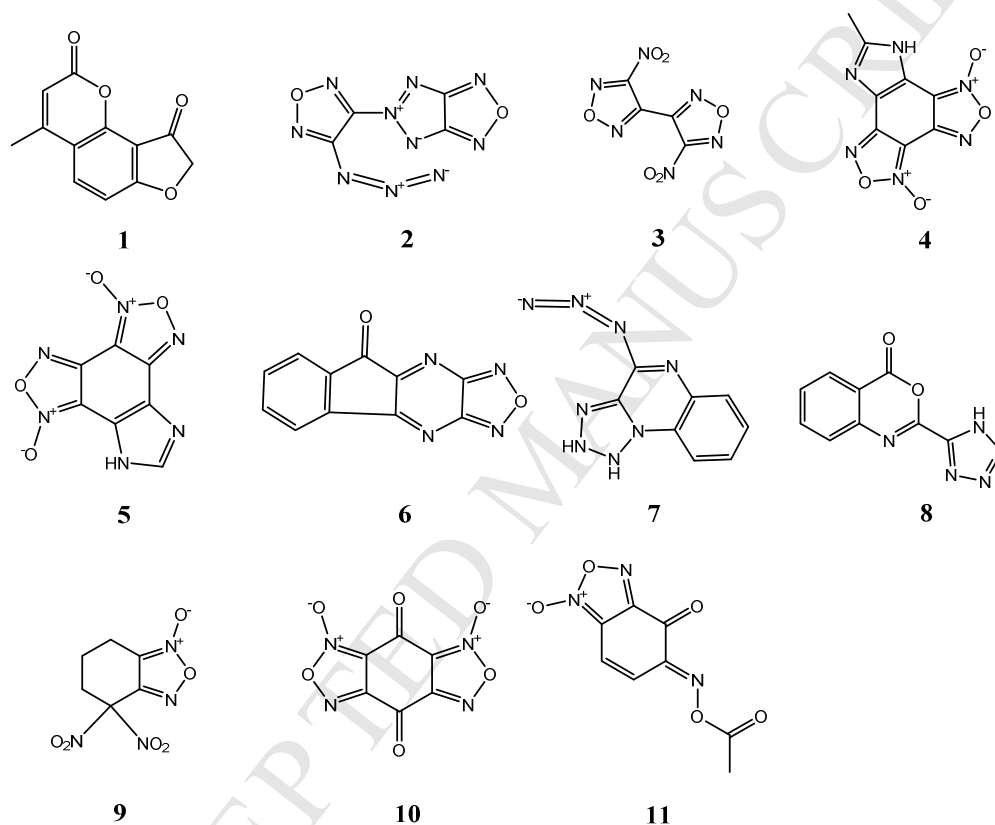
- a) edge-to-face π - π interaction with B:Phe44 and/or B:His53, and polar contacts with A:Ser127
- alternatively: b) edge-to-face π - π interaction with A:Tyr130, and polar contacts with GSH.

In this way, in the a) case, the interacting fragments could be optimized moving from the cytoplasmic to the most external part of the protein, reaching the external binding groove; in the b) case, the fragment could grow toward the cytoplasmic part, with the aim of establishing additional edge-to-face π - π interactions with B:Phe44 and/or B:His53.

The final stage of the workflow concerned the selection of the most promising fragments for the biological evaluation and the eventual subsequent structure-based chemical optimization (Step 6, Figure 2). The compounds identified for both the branches were then further visually inspected to check which positions could be modified without perturbing the original binding modes. 11 compounds (**1-11**, Chart 1) were finally selected, purchased and biologically tested. To assess the ability of compounds **1-11** (Chart 1) to interfere with the activity of mPGES-1, a cell-free assay using the microsomal fractions of interleukin-1 β (IL-1 β)-stimulated A549 cells (as source for mPGES-1) was applied. In a first screening round, all the compounds were solubilized in DMSO

and tested at a final concentration of 10 μ M. Biological data are summarized in Figure 3. Among the tested fragments, **6** (9H-indeno[1,2-b][1,2,5]oxadiazolo[3,4-e]pyrazin-9-one) showed the most promising inhibitory activity (~30% of inhibition), while interestingly, **3** and **11** showed only ~20% of inhibition (Figure 3).

Chart 1. Chemical structures of selected fragments **1-11**.



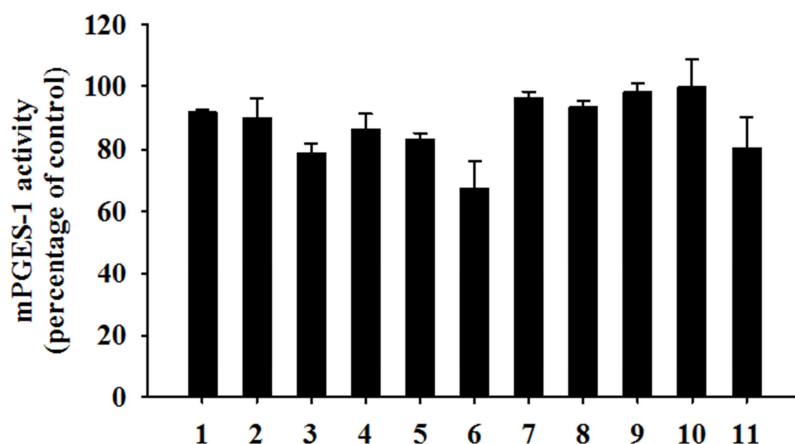


Figure 3. mPGES-1 remaining activity in the presence of compounds 1-11 at 10 μ M final concentration. Data are given as mean \pm S.E.M, n = 3. (1-column fitting image)

Fragment-to-lead optimization of compound 6 - Chemistry and biological evaluation. The most active identified fragment **6** was then modified following two distinct optimization schemes, starting from the analysis of the different binding modes from the two mPGES-1 structures considered for the docking calculations (*mpges_1_no_gsh* and *mpges_1_with_gsh* branches) (Figure 4).

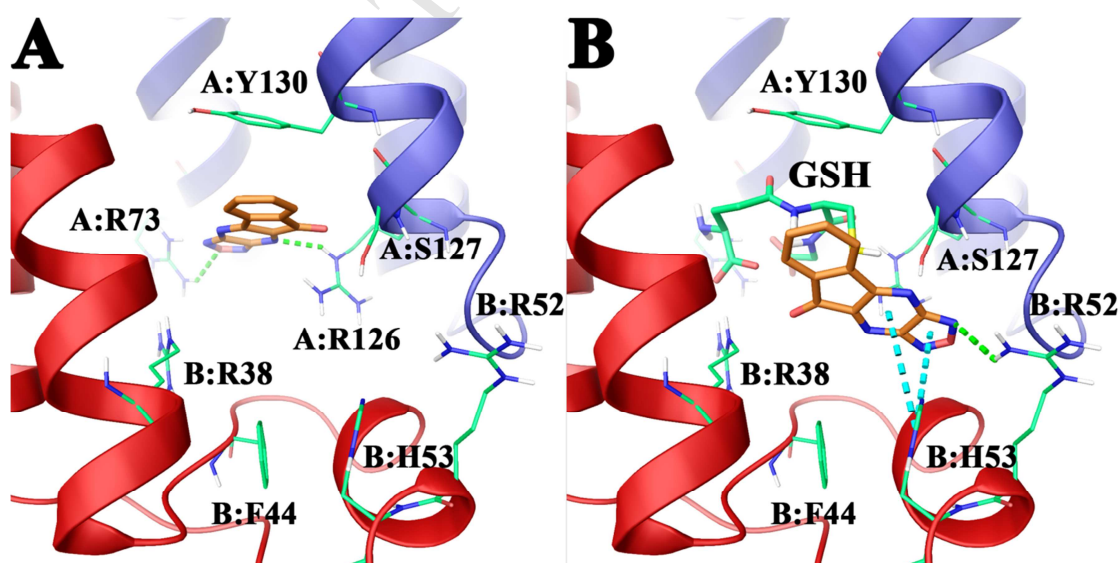


Figure 4. Different binding modes of **6** (colored by atom types: C orange, O red, N blue, polar H light gray) in the mPGES-1 binding site (represented in ribbons, blue for chain A, red for chain B) in the: a) absence, and b) presence of the cofactor (GSH). Residues in the active site are represented in sticks (colored by atom types: C green, N blue, O red, S yellow, H light gray, GSH depicted in green). H-bonds are represented in green dotted lines, while π - π interactions are depicted with cyan dotted lines. (2-column fitting image)

Firstly, following the hypothesis that the optimized derivatives could act as substrate/cofactor competitive inhibitors, we noticed that **6** occupied the cofactor binding site establishing the face-to-face with A:Tyr130 and two hydrogen bonds with A:Arg73 and A:Arg126 (Figure 4A), suggesting the introduction of chemical substituents able to fill the external part of the binding site.

Also, we carefully investigated the binding mode of **6** hypothesizing the substrate displacement and identifying two main binding modes in the GSH binding site (Figure 4B, Figure S1, Supporting Information). In the first one (Figure 4B), the oxadiazole moiety on ring D and the aromatic ring A of **6** established edge-to-face π - π interactions with B:Phe44 and B:His53, suggesting in this case the insertion of chemical groups able to making contacts with the residues belonging to the external binding groove (e.g. A:Tyr130). The alternative docking pose of **6** showed an edge-to-face π - π interaction with A:Tyr130, a π -cation with A:Arg126 and contacts with the cofactor GSH, while the remaining portion of the fragment pointed toward the cytoplasmic part of the protein (Figure S1, Supporting Information).

The analysis of the docking poses of the starting fragment **6** then showed that the insertion of substituents on the available positions of ring A could represent the starting point for the synthesis of optimized derivatives. With this aim, we developed a new and rapid synthetic route allowing the regioselective introduction of a hydroxyl as an attachment point on the aromatic

ring A of **6** (Scheme 1), specifically leading to its fragment derivatives **16**, **22**, **23**, prone to be modified for the optimization step.

In detail, substituted analogues of the tetracycle **6** were obtained by following the protocol described by the Bratton et al.[52] with appropriate modification to reduce the reaction times (Scheme 1). Namely, the synthesis of derivative **16** started from the electrophilic bromination of **12** with *N*-bromosuccinimide, followed by oxidation with dimethyl sulfoxide, to give the 7-substituted ninhydrin **13** in 60% yield.

Condensation of the latter with furazan-3,4-diamine (**14**) in a mixture of ethanol and acetic acid afforded the substituted tetracycle **15**. Although concomitant formation of the 4-substituted regioisomer of **15** was possible, this product was not isolated from the reaction mixture.

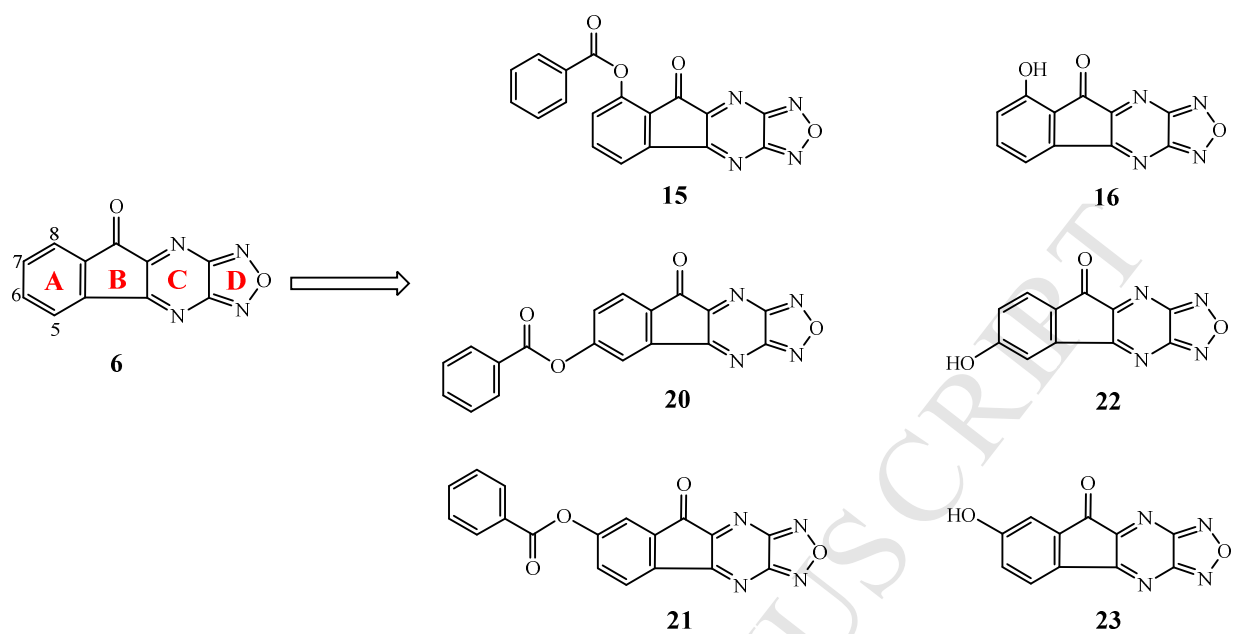
Indeed, the reaction of **15** with sodium thiophenolate in MeOH/THF (1:1) provided the phenol **16** in 95% yield. This deprotection was preferred to the one earlier reported, involving the use of cesium carbonate in tetrahydrofuran due to really shorter reaction time (from 5 days to only 2.5 h) with same yields[53]. It is noteworthy that the phenolic derivative **16** is useful for the introduction of additional functionality. In details, Mitsunobu reaction conditions could be employed for the introduction of a range of alkyl and aryl groups into the tetracycle obtained.

The procedure above described was exploited to obtain the isomeric C-6 and C-7 hydroxy substituted analogs. Therefore, after the protection of the hydroxyl group of the commercially available indanone **17** with benzoyl chloride[54], the synthetic strategy provided a mixture of two tetracycles **20** and **21** in ratio 1:0.88 respectively through the intermediate gem-diol **19**.

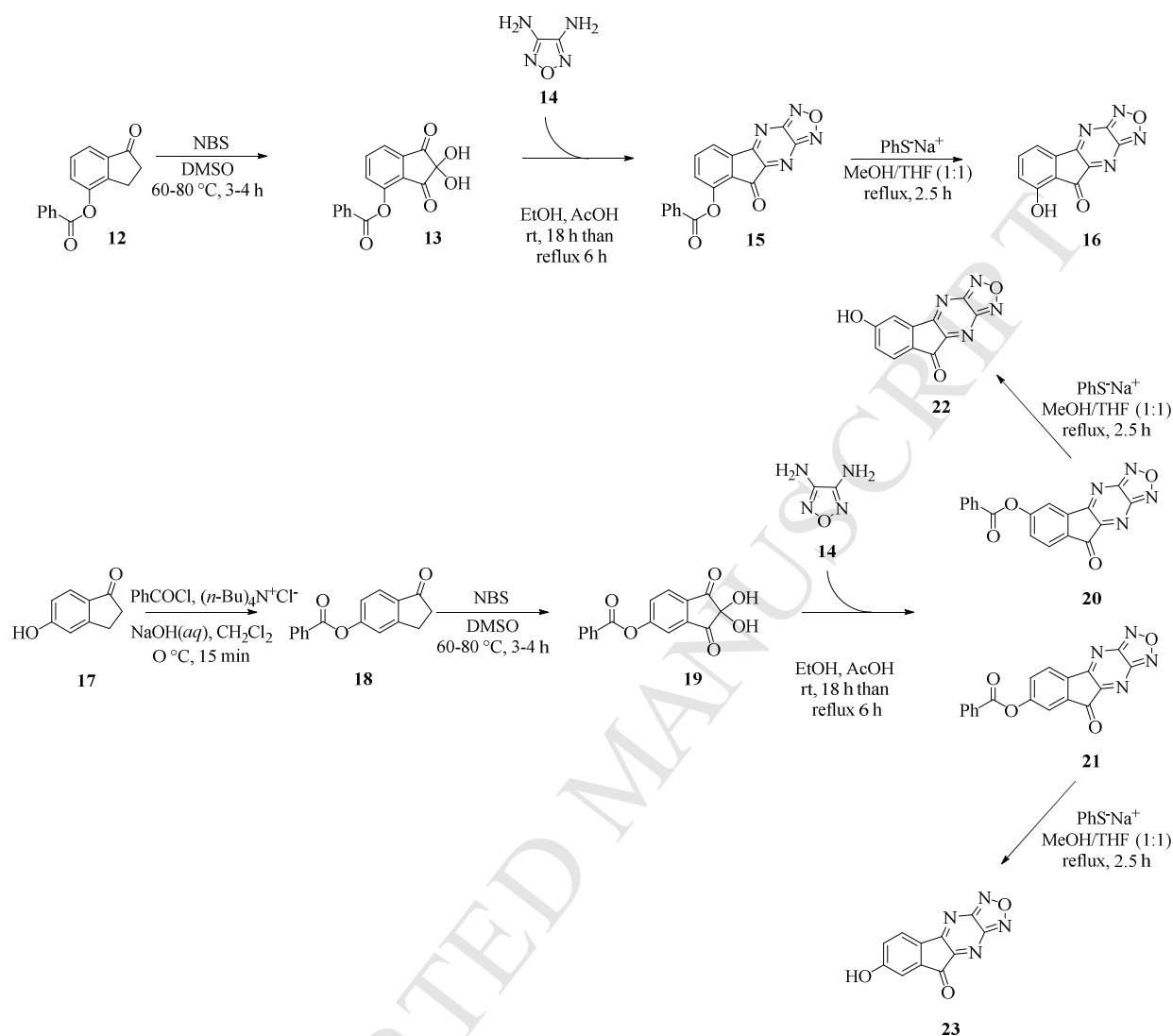
The two isomers were readily separated and purified by silica gel chromatography (Etp:AcOEt 7:3), then the ester cleavage produced the corresponding compounds **22** and **23** with a 95% yields in both cases.

We were intrigued by compounds **15**, **20**, **21** produced during the synthesis as the protected analogues of **16**, **22**, **23**, respectively, for which docking calculations showed promising binding modes in the mPGES-1 binding site. In particular, the ester function on ring A guaranteed the correct distance between the original core and the new aromatic function, and the gain of further favorable contacts while respecting the binding modes previously described for compound **6**. In details, in the absence of the cofactor we detected the growing of the starting fragment toward the external part of the binding site, with the establishment of an additional edge-to-face π - π interaction with with A:Phe44 for **16** (Figure 5A), and with A:Tyr130 (Figure 5B-C) for **20** and **21**. In the presence of the cofactor, compounds **15**, **20** and **21** confirmed the fundamental edge-to-face π - π interaction with B:Phe44/B:His53, respecting the binding mode of fragment **6** as reported in figure 4B. In addition, the attachment of the benzyloxy group on the ring A of **6** determined additional edge-to-face π - π interactions with A:Tyr130 (Figure 5D-F). Furthermore, we also found further binding modes of **15**, **20**, and **21** respecting the alternative docking pose of **6** (as reported in Figure S1, Supporting Information), in which the original core was oriented toward the A:Tyr130 (Figure S2, Supporting Information), while the benzyloxy substituents established edge-to-face π - π with B:Phe44/B:His53. Notably, in previous attempts[36] and after a retrospective analysis of the binding mode of the inhibitor LVJ[25, 36], we highlighted the importance of this key-interaction for the structure-based drug design and optimization of new mPGES-1 inhibitors. As expected, for compounds **16**, **22**, and **23** the insertion of the hydroxyl did not dramatically perturb the proposed binding modes of the starting fragment **6** (Figure S3, Supporting Information).

Chart 2. Chemical structure of compounds **6**, **15**, **16**, **20-23**.



Scheme 1. Chemical synthesis of compounds **15**, **16**, **20-23**.



Results from the assessment of mPGES-1 inhibition by compounds **15**, **16**, **20-23** corroborated the computational outcomes, and specifically compounds **15**, **20** and **21** confirmed their ability to interfere with mPGES-1 activity (% of inhibition: ~ 70% for **15**; ~ 70% for **20**; ~ 85% for **21**, at 10 μ M). The related IC₅₀ values substantiate these results, obtaining promising IC₅₀ values in the low micromolar range (IC₅₀ = 4.6 \pm 0.2 μ M for **15**; IC₅₀ = 2.4 \pm 1.0 μ M for **20**; IC₅₀ = 2.4 \pm 0.8 μ M for **21**) (Figure 6). As expected, compounds **16**, **22**, and **23** showed an inhibitory activity comparable with that of starting fragment **6** (% of inhibition = 30% for **22**, 15% for **23**, tested at 10 μ M), while a lower value was found for **16** (5% of inhibition at 10 μ M).

From a structural point of view, the here reported novel mPGES-1 inhibitors were discovered performing molecular docking experiments on both the protein forms in the absence and in the presence of the cofactor (glutathione, GSH). In parallel, new experimental information arose from the analysis of the recently released crystal structures of mPGES-1 co-complexed with high affinity inhibitors (PDB codes: 4BPM, 4WAB, 4YK5, 4YL0, 4YL1, 4YL3, 5BQG, 5BQH, 5BQI), confirming the presence of GSH at its site. Furthermore, the only one co-crystallized inhibitor acting as partial substrate/cofactor competitor (PDB code: 4AL1) is a close analogue of GSH (bis-phenyl-GSH), thus maintaining the same network of interactions of the original cofactor at its site. Taken together, these experimental data point out that the displacement of the cofactor is possible only if the binding site is occupied by a similar ligand respecting the binding mode reported for GSH. These structural outcomes indicate the substrate displacement hypothesis for the set of compounds here reported, and these information will be accounted for the future *in silico* design of optimized derivatives.

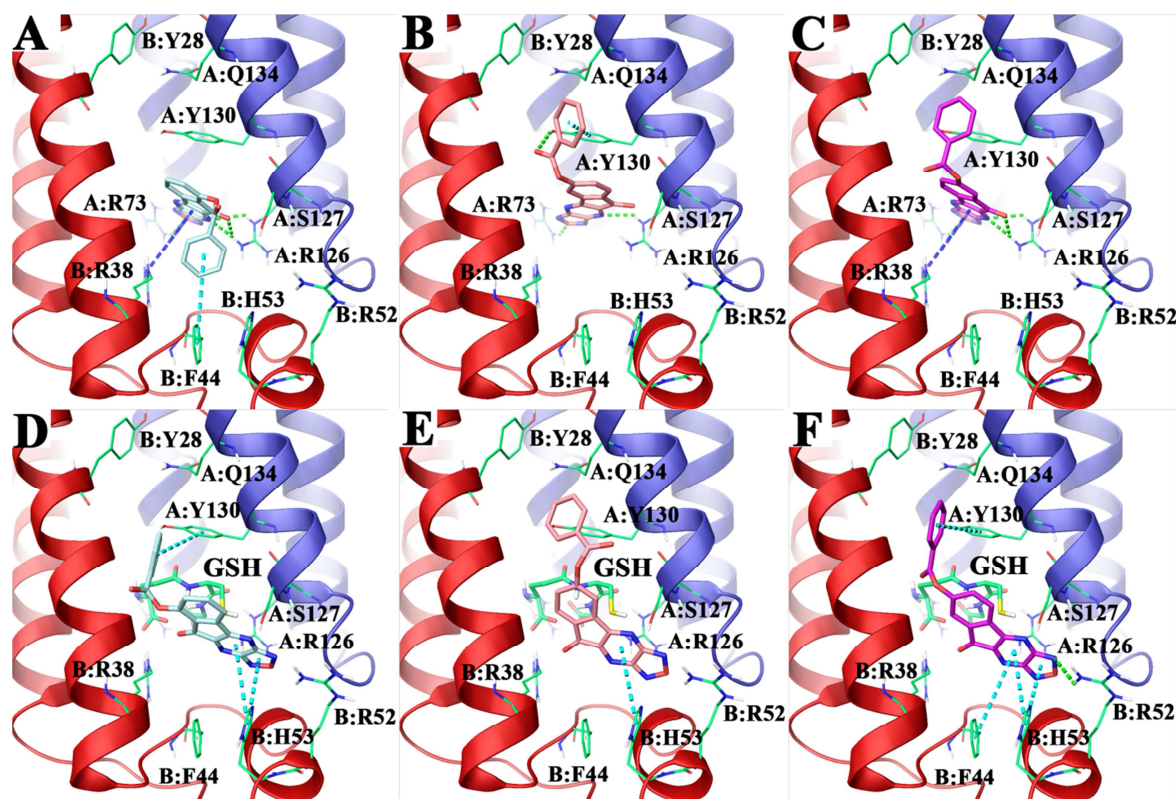


Figure 5. a,d) 3D docking models of **15** (colored by atom types: C cyan, O red, N blue, polar H light gray); b,e) **20** (colored by atom types: C pink, O red, N blue, polar H light gray), and c,f) **21** (colored by atom types: C violet, O red, N blue, polar H light gray) in the mPGES-1 binding site in the absence (a,b,c) and in the presence (d,e,f) of the cofactor GSH. Residues in the active site are represented in sticks (colored by atom types: C green, N blue, O red, S yellow, H light gray). H-bonds are represented in green dotted lines, while π - π interactions are depicted with cyan dotted lines. (2-column fitting image)

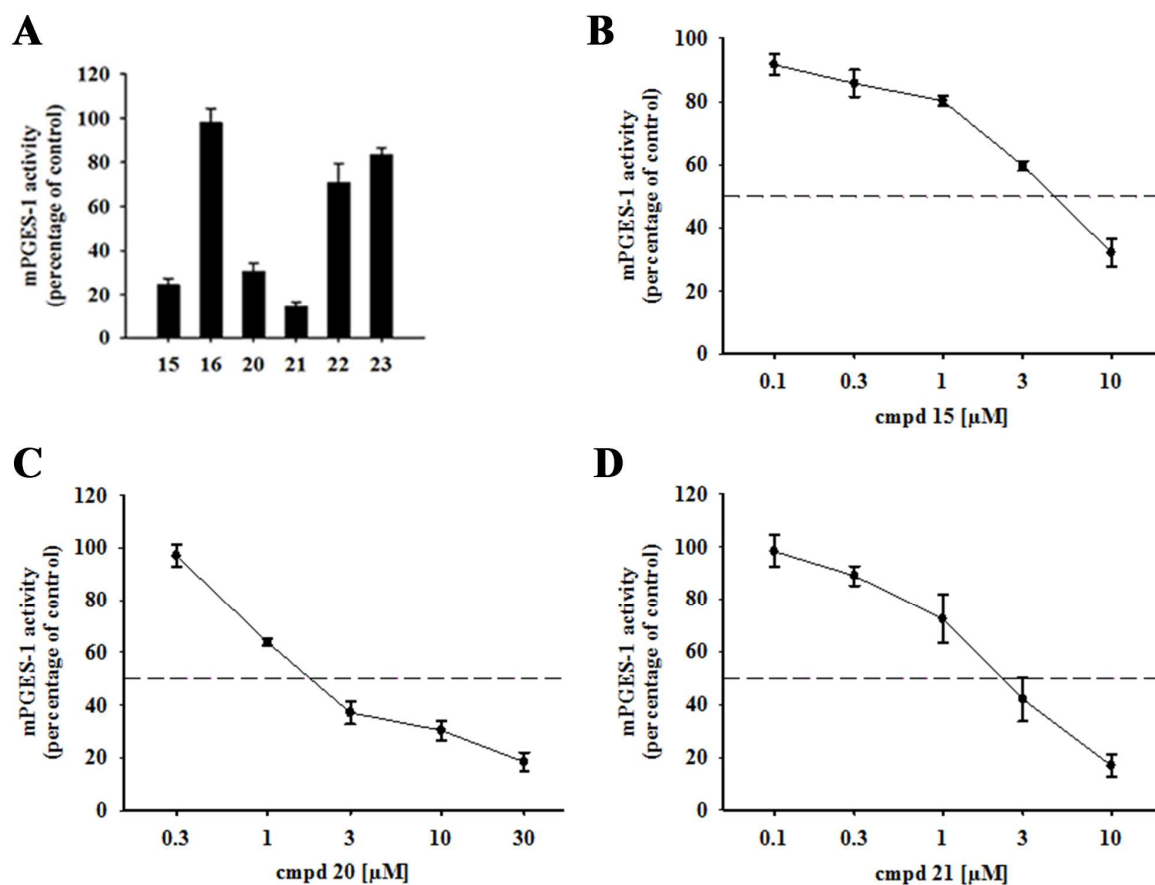


Figure 6. a) mPGES-1 remaining activity in the presence of compounds **15**, **16**, **20-23** at 10 μ M final concentration. b, c, d) Concentration-response curves of compounds **15**, **20**, **21** for inhibition of mPGES-1 activity, respectively. Data are given as mean \pm S.E.M., n = 3. (2-column fitting image)

Conclusion

Here we reported about the computer-aided identification, biological evaluation, and optimization of the novel mPGES-1 small fragment inhibitor **6** following a Fragment Virtual Screening approach.

In detail, from a multi-step Fragment Virtual Screening 11 compounds were selected, purchased and biologically evaluated. Starting from the most active fragment **6** (~30% of inhibition at concentration of 10 μ M), we have developed a synthetic route aimed at the

preparation of its derivatives **16**, **22**, and **23**, with the introduction of a hydroxy substituent in different positions as possible attachment points for the future optimization steps.

By means of docking calculations, we also evaluated the binding modes of the synthesized protected analogues **15**, **20**, and **21** featuring a benzyloxy chemical function attached to the original chemical core. Computational data showed the ability of these compounds of gaining several interactions while not affecting the original binding modes of **6**. Encouraged by the computational results, we biologically evaluated **15**, **20**, and **21** *in vitro*, revealing promising inhibitory activities against mPGES-1 in the low micromolar range ($IC_{50} = 4.6 \pm 0.2 \mu\text{M}$ for **15**; $IC_{50} = 2.4 \pm 1.0$ for **20**; $IC_{50} = 2.4 \pm 0.8 \mu\text{M}$ for **21**), disclosing **6** as a new interesting chemical core for the development of mPGES-1 inhibitors.

Thanks to the rapid and efficient synthetic route developed, these results pave the way for the design of new inhibitors, firstly considering the possibility of attaching a large set of substituents, exploiting the hydroxy groups introduced on the different available positions on ring A of **6**. Furthermore, different substitution patterns on the terminal aromatic function belonging to the benzyloxy substituent will be also evaluated. Moreover, the data here shown will provide valuable information for the design of further optimized derivatives as novel mPGES-1 inhibitors for the treatment of cancer and inflammation.

ASSOCIATED CONTENT

Supporting Information. NMR data, and docking models. This material is available free of charge via the Internet at <http://pubs.acs.org>.

AUTHOR INFORMATION

Corresponding Author

*To whom correspondence should be addressed: bifulco@unisa.it, Telephone: +39 (0)89 969741, Fax: +39 (0)89 969602; pcampiglia@unisa.it, Telephone: +39 (0)89 969242, Fax: +39 (0)89 962804

Author Contributions

The manuscript was written through contributions of all authors. All authors have given approval to the final version of the manuscript.

Funding Sources

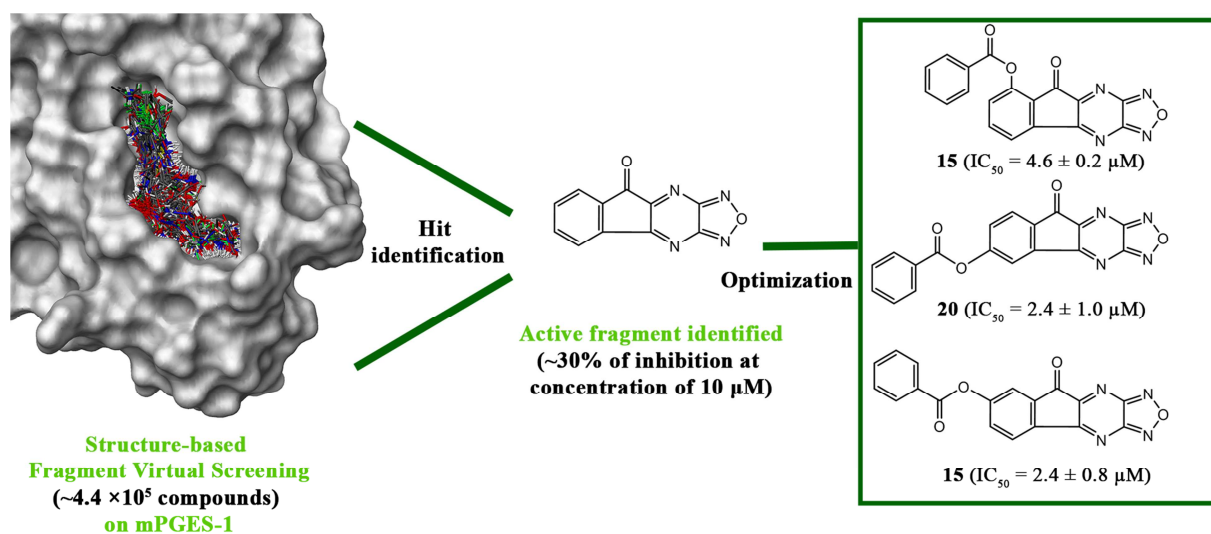
This work was supported by the University of Salerno (Italy), and by the Associazione Italiana per la Ricerca sul Cancro (AIRC) (grants IG 2012—IG_12777 and IG 2015—IG_17440 to Bifulco Giuseppe).

Notes

ACKNOWLEDGMENT

G.L. acknowledges fellowship support from Associazione Italiana per la Ricerca sul Cancro (AIRC) (grant IG 2012—IG_12777).

Graphical abstract



REFERENCES

- [1] D. Wang, R.N. Dubois, Prostaglandins and cancer, *Gut*, 55 (2006) 115-122.
- [2] L.M. Coussens, Z. Werb, Inflammation and cancer, *Nature*, 420 (2002) 860-867.
- [3] E. Elinav, R. Nowarski, C.A. Thaiss, B. Hu, C. Jin, R.A. Flavell, Inflammation-induced cancer: crosstalk between tumours, immune cells and microorganisms, *Nat. Rev. Cancer*, 13 (2013) 759-771.
- [4] F. Colotta, P. Allavena, A. Sica, C. Garlanda, A. Mantovani, Cancer-related inflammation, the seventh hallmark of cancer: links to genetic instability, *Carcinogenesis*, 30 (2009) 1073-1081.
- [5] I. Rothman, J.L. Stanford, A. Kuniyuki, R.E. Berger, Self-report of prostatitis and its risk factors in a random sample of middle-aged men, *Urology*, 64 (2004) 876-879.
- [6] E.V. Loftus, Jr., Epidemiology and risk factors for colorectal dysplasia and cancer in ulcerative colitis, *Gastroenterol. Clin. North Am.*, 35 (2006) 517-531.
- [7] K.A. Rosenblatt, K.G. Wicklund, J.L. Stanford, Sexual factors and the risk of prostate cancer, *Am. J. Epidemiol.*, 153 (2001) 1152-1158.
- [8] S. Rakoff-Nahoum, Why cancer and inflammation?, *Yale J. Biol. Med.*, 79 (2006) 123-130.
- [9] K.D. Rainsford, Profile and mechanisms of gastrointestinal and other side effects of nonsteroidal anti-inflammatory drugs (NSAIDs), *Am. J. Med.*, 107 (1999) 27S-35S.
- [10] P. McGettigan, D. Henry, Cardiovascular risk and inhibition of cyclooxygenase: a systematic review of the observational studies of selective and nonselective inhibitors of cyclooxygenase 2, *JAMA*, 296 (2006) 1633-1644.
- [11] Y. Cheng, M. Wang, Y. Yu, J. Lawson, C.D. Funk, G.A. Fitzgerald, Cyclooxygenases, microsomal prostaglandin E synthase-1, and cardiovascular function, *J. Clin. Invest.*, 116 (2006) 1391-1399.
- [12] I. Kudo, M. Murakami, Prostaglandin E synthase, a terminal enzyme for prostaglandin E2 biosynthesis, *J. Biochem. Mol. Biol.*, 38 (2005) 633-638.

- [13] A. Koeberle, O. Werz, Perspective of microsomal prostaglandin E synthase-1 as drug target in inflammation-related disorders, *Biochem. Pharmacol.*, 98 (2015) 1-15.
- [14] B. Samuelsson, R. Morgenstern, P.J. Jakobsson, Membrane prostaglandin E synthase-1: a novel therapeutic target, *Pharmacol. Rev.*, 59 (2007) 207-224.
- [15] D. Kamei, K. Yamakawa, Y. Takegoshi, M. Mikami-Nakanishi, Y. Nakatani, S. Oh-Ishi, H. Yasui, Y. Azuma, N. Hirasawa, K. Ohuchi, H. Kawaguchi, Y. Ishikawa, T. Ishii, S. Uematsu, S. Akira, M. Murakami, I. Kudo, Reduced pain hypersensitivity and inflammation in mice lacking microsomal prostaglandin e synthase-1, *J. Biol. Chem.*, 279 (2004) 33684-33695.
- [16] D. Engblom, S. Saha, L. Engstrom, M. Westman, L.P. Audoly, P.J. Jakobsson, A. Blomqvist, Microsomal prostaglandin E synthase-1 is the central switch during immune-induced pyresis, *Nat. Neurosci.*, 6 (2003) 1137-1138.
- [17] M. Westman, M. Korotkova, E. af Klint, A. Stark, L.P. Audoly, L. Klareskog, A.K. Ulfgren, P.J. Jakobsson, Expression of microsomal prostaglandin E synthase 1 in rheumatoid arthritis synovium, *Arthritis Rheum.*, 50 (2004) 1774-1780.
- [18] H. Fahmi, mPGES-1 as a novel target for arthritis, *Curr. Opin. Rheumatol.*, 16 (2004) 623-627.
- [19] C.E. Trebino, J.L. Stock, C.P. Gibbons, B.M. Naiman, T.S. Wachtmann, J.P. Umland, K. Pandher, J.M. Lapointe, S. Saha, M.L. Roach, D. Carter, N.A. Thomas, B.A. Durtschi, J.D. McNeish, J.E. Hambor, P.J. Jakobsson, T.J. Carty, J.R. Perez, L.P. Audoly, Impaired inflammatory and pain responses in mice lacking an inducible prostaglandin E synthase, *Proc. Natl. Acad. Sci. U. S. A.*, 100 (2003) 9044-9049.
- [20] D. Kamei, M. Murakami, Y. Nakatani, Y. Ishikawa, T. Ishii, I. Kudo, Potential role of microsomal prostaglandin E synthase-1 in tumorigenesis, *J. Biol. Chem.*, 278 (2003) 19396-19405.
- [21] M. Nakanishi, V. Gokhale, E.J. Meuillet, D.W. Rosenberg, mPGES-1 as a target for cancer suppression A comprehensive invited review "Phospholipase A(2) and lipid mediators", *Biochimie*, 92 (2010) 660-664.
- [22] A. Koeberle, S.A. Laufer, O. Werz, Design and Development of Microsomal Prostaglandin E Synthase-1 Inhibitors: Challenges and Future Directions, *J. Med. Chem.*, (2016) in press.
- [23] H.-H. Chang, E.J. Meuillet, Identification and development of mPGES-1 inhibitors: where we are at?, *Future Med. Chem.*, 3 (2011) 1909-1934.
- [24] T. Sjogren, J. Nord, M. Ek, P. Johansson, G. Liu, S. Geschwindner, Crystal structure of microsomal prostaglandin E-2 synthase provides insight into diversity in the MAPEG superfamily, *Proc. Natl. Acad. Sci. U. S. A.*, 110 (2013) 3806-3811.
- [25] D. Li, N. Howe, A. Dukupati, S.T.A. Shah, B.D. Bax, C. Edge, A. Bridges, P. Hardwicke, O.M.P. Singh, G. Giblin, A. Pautsch, R. Pfau, G. Schnapp, M. Wang, V. Olieric, M. Caffrey, Crystallizing Membrane Proteins in the Lipidic Mesophase. Experience with Human Prostaglandin E2 Synthase 1 and an Evolving Strategy, *Cryst. Growth Des.*, 14 (2014) 2034-2047.
- [26] J.G. Luz, S. Antonysamy, S.L. Kuklish, B. Condon, M.R. Lee, D. Allison, X.P. Yu, S. Chandrasekhar, R. Backer, A. Zhang, M. Russell, S.S. Chang, A. Harvey, A.V. Sloan, M.J. Fisher, Crystal Structures of mPGES-1 Inhibitor Complexes Form a Basis for the Rational Design of Potent Analgesic and Anti-Inflammatory Therapeutics, *J. Med. Chem.*, 58 (2015) 4727-4737.
- [27] T. Weinert, V. Olieric, S. Waltersperger, E. Panepucci, L. Chen, H. Zhang, D. Zhou, J. Rose, A. Ebihara, S. Kuramitsu, D. Li, N. Howe, G. Schnapp, A. Pautsch, K. Bargsten, A.E.

- Prota, P. Surana, J. Kottur, D.T. Nair, F. Basilico, V. Cecatiello, S. Pasqualato, A. Boland, O. Weichenrieder, B.C. Wang, M.O. Steinmetz, M. Caffrey, M. Wang, Fast native-SAD phasing for routine macromolecular structure determination, *Nat. Methods*, 12 (2015) 131-133.
- [28] M.A. Schiffler, S. Antonysamy, S.N. Bhattachar, K.M. Campanale, S. Chandrasekhar, B. Condon, P.V. Desai, M.J. Fisher, C. Groshong, A. Harvey, M.J. Hickey, N.E. Hughes, S.A. Jones, E.J. Kim, S.L. Kuklish, J.G. Luz, B.H. Norman, R.E. Rathmell, J.R. Rizzo, T.W. Seng, S.J. Thibodeaux, T.A. Woods, J.S. York, X.P. Yu, Discovery and Characterization of 2-Acylaminoimidazole Microsomal Prostaglandin E Synthase-1 Inhibitors, *J. Med. Chem.*, 59 (2015) 194-205.
- [29] M.D. Guerrero, M. Aquino, I. Bruno, M.C. Terencio, M. Paya, R. Riccio, L. Gomez-Paloma, Synthesis and pharmacological evaluation of a selected library of new potential anti-inflammatory agents bearing the gamma-hydroxybutenolide scaffold: a new class of inhibitors of prostanoid production through the selective modulation of microsomal prostaglandin E synthase-1 expression, *J. Med. Chem.*, 50 (2007) 2176-2184.
- [30] M. Aquino, M.D. Guerrero, I. Bruno, M.C. Terencio, M. Paya, R. Riccio, Development of a second generation of inhibitors of microsomal prostaglandin E synthase 1 expression bearing the gamma-hydroxybutenolide scaffold, *Bioorg. Med. Chem.*, 16 (2008) 9056-9064.
- [31] R. De Simone, R.M. Andres, M. Aquino, I. Bruno, M.D. Guerrero, M.C. Terencio, M. Paya, R. Riccio, Toward the discovery of new agents able to inhibit the expression of microsomal prostaglandin E synthase-1 enzyme as promising tools in drug development, *Chem. Biol. Drug Des.*, 76 (2010) 17-24.
- [32] R. De Simone, M.G. Chini, I. Bruno, R. Riccio, D. Mueller, O. Werz, G. Bifulco, Structure-Based Discovery of Inhibitors of Microsomal Prostaglandin E-2 Synthase-1, 5-Lipoxygenase and 5-Lipoxygenase-Activating Protein: Promising Hits for the Development of New Anti-inflammatory Agents, *J. Med. Chem.*, 54 (2011) 1565-1575.
- [33] M.G. Chini, R. De Simone, I. Bruno, R. Riccio, F. Dehm, C. Weinigel, D. Barz, O. Werz, G. Bifulco, Design and synthesis of a second series of triazole-based compounds as potent dual mPGES-1 and 5-lipoxygenase inhibitors, *Eur. J. Med. Chem.*, 54 (2012) 311-323.
- [34] G. Lauro, M. Strocchia, S. Terracciano, I. Bruno, K. Fischer, C. Pergola, O. Werz, R. Riccio, G. Bifulco, Exploration of the dihydropyrimidine scaffold for the development of new potential anti-inflammatory agents blocking prostaglandin E-2 synthase-1 enzyme (mPGES-1), *Eur. J. Med. Chem.*, 80 (2014) 407-415.
- [35] M.G. Chini, C. Ferroni, V. Cantone, P. Dambruoso, G. Varchi, A. Pepe, K. Fischer, C. Pergola, O. Werz, I. Bruno, R. Riccio, G. Bifulco, Elucidating new structural features of the triazole scaffold for the development of mPGES-1 inhibitors, *MedChemComm*, 6 (2015) 75-79.
- [36] S. Terracciano, G. Lauro, M. Strocchia, K. Fischer, O. Werz, R. Riccio, I. Bruno, G. Bifulco, Structural Insights for the Optimization of Dihydropyrimidin-2(1H)-one Based mPGES-1 Inhibitors, *ACS Med. Chem. Lett.*, 6 (2015) 187-191.
- [37] G. Lauro, P. Tortorella, A. Bertamino, C. Ostacolo, A. Koeberle, K. Fischer, I. Bruno, S. Terracciano, I.M. Gomez-Monterrey, M. Tauro, F. Loiodice, E. Novellino, R. Riccio, O. Werz, P. Campiglia, G. Bifulco, Structure-Based Design of Microsomal Prostaglandin E Synthase-1 (mPGES-1) Inhibitors using a Virtual Fragment Growing Optimization Scheme, *ChemMedChem*, 11 (2016) 612-619.
- [38] S. Di Micco, C. Spatafora, N. Cardullo, R. Riccio, K. Fischer, C. Pergola, A. Koeberle, O. Werz, M. Chalal, D. Vervandier-Fasseur, C. Tringali, G. Bifulco, 2,3-Dihydrobenzofuran

- privileged structures as new bioinspired lead compounds for the design of mPGES-1 inhibitors, *Bioorg. Med. Chem.*, 24 (2016) 820-826.
- [39] M. Iranshahi, M.G. Chini, M. Masullo, A. Sahebkar, A. Javidnia, M. Chitsazian Yazdi, C. Pergola, A. Koeberle, O. Werz, C. Pizza, S. Terracciano, S. Piacente, G. Bifulco, Can Small Chemical Modifications of Natural Pan-inhibitors Modulate the Biological Selectivity? The Case of Curcumin Prenylated Derivatives Acting as HDAC or mPGES-1 Inhibitors, *J. Nat. Prod.*, 78 (2015) 2867-2879.
- [40] D.E. Scott, A.G. Coyne, S.A. Hudson, C. Abell, Fragment-based approaches in drug discovery and chemical biology, *Biochemistry*, 51 (2012) 4990-5003.
- [41] D.C. Rees, M. Congreve, C.W. Murray, R. Carr, Fragment-based lead discovery, *Nat. Rev. Drug Discov.*, 3 (2004) 660-672.
- [42] J.J. Irwin, B.K. Shoichet, ZINC--a free database of commercially available compounds for virtual screening, *J. Chem. Inf. Model.*, 45 (2005) 177-182.
- [43] J.J. Irwin, T. Sterling, M.M. Mysinger, E.S. Bolstad, R.G. Coleman, ZINC: a free tool to discover chemistry for biology, *J. Chem. Inf. Model.*, 52 (2012) 1757-1768.
- [44] N.M. O'Boyle, M. Banck, C.A. James, C. Morley, T. Vandermeersch, G.R. Hutchison, Open Babel: An open chemical toolbox, *J. Cheminform.*, 3 (2011) 33.
- [45] Maestro, version 10.2, Schrödinger, LLC, New York, NY, (2015).
- [46] O. Trott, A.J. Olson, Software News and Update AutoDock Vina: Improving the Speed and Accuracy of Docking with a New Scoring Function, Efficient Optimization, and Multithreading, *J. Comput. Chem.*, 31 (2010) 455-461.
- [47] W. Humphrey, A. Dalke, K. Schulten, VMD: visual molecular dynamics, *J. Mol. Graph.*, 14 (1996) 33-38, 27-38.
- [48] A. Koeberle, U. Siemoneit, U. Buehring, H. Northoff, S. Laufer, W. Albrecht, O. Werz, Licofelone suppresses prostaglandin E(2) formation by interference with the inducible microsomal prostaglandin E(2) synthase-1, *J. Pharmacol. Exp. Ther.*, 326 (2008) 975-982.
- [49] S. He, L. Lai, Molecular docking and competitive binding study discovered different binding modes of microsomal prostaglandin E synthase-1 inhibitors, *J. Chem. Inf. Model.*, 51 (2011) 3254-3261.
- [50] C. Abad-Zapatero, Ligand efficiency indices for effective drug discovery, *Expert Opin. Drug Discov.*, 2 (2007) 469-488.
- [51] C.A. Lipinski, F. Lombardo, B.W. Dominy, P.J. Feeney, Experimental and computational approaches to estimate solubility and permeability in drug discovery and development settings, *Adv. Drug Deliv. Rev.*, 46 (2001) 3-26.
- [52] L.D. Bratton, P.C. Unangst, J.R. Rubin, B.K. Trivedi, Preparation of 6-, 7-, and 9-substituted derivatives of 2-oxa-1,3,4,10-tetraazacyclopenta[b]fluoren-9-one, *J. Heterocycl. Chem.*, 38 (2001) 1103-1111.
- [53] R.N. MacCoss, D.J. Henry, C.T. Brain, S.V. Ley, Catalytic polymer-supported potassium thiophenolate in methanol as a method for the removal of ester, amide, and thioacetate protecting groups, *Synlett*, (2004) 675-678.
- [54] A.M. Simion, I. Hashimoto, Y. Mitoma, N. Egashira, C. Simion, O-Acylation of Substituted Phenols with Various Alkanoyl Chlorides under Phase-Transfer Catalyst Conditions, *Synth. Commun.*, 42 (2012) 921-931.

HIGHLIGHTS:

- New mPGES-1 inhibitors were identified using a Fragment Virtual Screening approach
- The active fragment **6** was optimized by means of molecular docking experiments
- A new chemical procedure was developed for synthesizing the optimized compounds
- Compounds **15**, **20** and **21** inhibit mPGES-1 in the low micromolar range